www.czasopisma.pan.pl PAN www.journals.pan.pl
POLSKA AKADEMIA NAUK

Arch. Metall. Mater. **65** (2020), 4, 1297-1301

DOI: 10.24425/amm.2020.133688

KWANGMIN LEE[1*], GUNHEE LEE[2]

MECHANICAL PROPERTIES AND CORROSION BEHAVIORS OF AGED Ti-4Mo-4Cr-X (X = Sn, V, Zr) ALLOYS FOR METALLIC BIOMATERIALS

The purpose of this study was to investigate the mechanical properties of beta type aged Ti-4Mo-4Cr-X (X = V, Sn, Zr) quaternary alloy for use as a cardiovascular stent. Titanium (Ti) alloys were fabricated using a vacuum arc remelting furnace process. To homogenize the specimens of each composition and remove the micro segregation, all cast specimens were subjected to homogenization at 850°C for 4 h, which was 100°C higher than the β-transus temperature of 750°C. The tensile strength and elongation of the aged Ti-4Mo-4Cr-X (X = V, Sn, Zr) alloys were increased as compared to the homogenized alloys. In addition, many α/β interface boundaries formed after aging treatment at 450°C, which acted as inhibitors of strain and caused an increase in tensile strength. The elongation of Ti-4Mo-4Cr-X alloys consisting of α + β phases after aging treatment was improved by greater than 30%. Results of a potentiodynamic polarization test showed that the lowest current density of Ti-4Mo-4Cr-4Sn with 1.05×10^{-8} A/cm^2 was obtained. The present Ti-4Mo-4Cr-X alloys showed better corrosion characteristics as compared to the 316L stainless steel and L605 (Co-Cr alloy) cardiovascular stent alloys.

Keywords: Beta Ti-alloy, Metallic biomaterials, Aging, Potentiodynamic polarization

1. Introduction

Research on the development of titanium (Ti)-based stent materials for blood vessels has been rarely conducted. Ti-based alloys for bare-metal stents are extremely attractive because of their high strength, low elastic modulus, excellent corrosion resistance, and superior biocompatibility [1]. An ideal bare metal stent has a low profile, good expandability ratio, sufficient radial hoop strength, negligible recoil, and sufficient flexibility [2].

Ti alloys are designed by alloying quantities of α- and β-stabilizing elements. Thus, the fractions of α and β phases are determined by the alloying elements [3]. Beta-phase stabilizers including Mo, Cr, Nb, Mn, Co, and Fe have been studied for biomedical applications. The molybdenum equivalence (Mo_{eq}) in the range of 12-15 wt.% has been reported as an optimal combination of strength and toughness [4].

Ti alloy performance is strongly dependent on the controlled thermomechanical treatment [5]. Further plastic deformation, including texture evolution, and aging treatment result in grain refinement and second-phase precipitation, which are required for the strength-ductility trade-off [6]. This study investigated the mechanical properties and corrosion behaviors in Ringer's solution of a beta-type aged Ti-4Mo-4Cr-X (X = V, Sn, Zr) quaternary alloy for use as a cardiovascular stent.

2. Experimental

Ingots of Ti-4Mo-4Cr-X (X = 2, 3, 4 wt.% V, 2, 3, 4 wt.% Sn, and 2, 3, 4 wt.% Zr) quaternary alloys were fabricated through a vacuum arc remelting (VAR, ACE VACUUM, AVA-1500, Korea). Commercially pure Ti chips (ASTM CP Grade II), Mo bars (99.8 wt.%), Cr chips (99.9 wt.%), V sheets (99.9 wt.%), Sn balls (99.9 wt.%), and Zr sheets (99.9 wt.%) were arc melted in a water-cooled copper hearth with a tungsten electrode. The ingots were remelted four times under an argon atmosphere and hot forged with a thickness reduction of 35% to ensure chemical homogeneity. All cast ingots were then homogenized at 850°C for 4 h, which was 100°C higher than the β-transus temperature of 750°C. In addition, aging treatment was conducted at 450°C for 16 h.

The phase constitutions of the alloys were examined by X-ray diffraction (XRD, PANalytical, X' Pert pro, Netherland) analysis using Cu-Kα radiation over 2θ range from 30-90° at

[1] CHONNAM NATIONAL UNIVERSITY, SCHOOL OF MATERIALS SCIENCE & ENGINEERING, GWANGJU, REPUBLIC OF KOREA
[2] 21CENTURY MEDICAL CO. LTD., GWANGJU, KOREA

* Corresponding author: kmlee@jnu.ac.kr

an accelerating voltage of 40 kV, a current of 250 mA, and a scanning speed of 2°/min. Tensile specimens were manufactured in accordance with the ASTM E8 standard. A tensile test was conducted using a universal material tester (Shimadzu: AG-100KNIC) at a load of 20,000 N under a tensile load of 10 mm/min. The fractography after the tensile test was examined using a scanning electron microscope (S-4700, HITACHI, Japan). Electrochemical experiments were performed on a flat cell corrosion tester (PARSTAT 2273, USA) at a temperature of 37±1°C. A three-electrode cell was used for potentiodynamic polarization tests, where the reference electrode was a silver–silver chloride electrode, the counter electrode was made of a platinum plate, and the specimen was the working electrode. All experiments were conducted at a constant scan rate of 0.25 mV/s, initiated at −250 mV below the open-circuit potential. The working electrolyte was Ringer's physical solution.

3. Results and discussion

Fig. 1 shows the XRD patterns of the aged (a) Ti-4Mo-4Cr-*x*V (*x* = 2, 3, 4) alloys, (b) Ti-4Mo-4Cr-*x*Sn (*x* = 2, 3, 4) alloys, and (c) Ti-4Mo-4Cr-*x*Zr (*x* = 2, 3, 4) alloys. The Ti-4Mo-4Cr-(2, 3, 4) V alloys showed that β-phase peaks formed in the (110), (200) and (211) planes. It was also observed that α-phase peaks formed in the (100), (002), (102) and (110) planes in the alloys containing 2 wt.% and 3 wt.% V. The Ti-4Mo-4Cr-4V alloy nearly showed stable β-phase peaks because of a higher value of Mo_{eq} (12.2). The beta phase stability in Ti-4Mo-4Cr-*x*V (*x* = 2, 3, 4) alloys also increased with increasing V content. By contrast, the α-phase peaks of aged Ti-4Mo-4Cr-*x*Zr (*x* = 2, 3, 4) alloys were found to be higher than those of homogenized specimens, suggesting that precipitation of α phases increased with aging treatment. The precipitation of α phases could be attributed to the existence of α″ phases at the grain boundaries, which acted as precursor nucleation sites for the stable α phases.

Fig. 2 shows the stress-strain curves after tensile testing of Ti-4Mo-4Cr-X (X = V, Sn, Zr), which were homogenized at 850°C for 4 h and subsequently aging treated at 450°C for 16 h. As shown in Fig. 2, the tensile strength of the aged Ti-4Mo-4Cr-X (X = V, Sn) alloys increased with increasing V or Sn content. The maximum tensile strength for the Ti-4Mo-4Cr-4Sn alloy was approximately 1554 MPa with an elongation of 38%. The tensile strength of Ti-4Mo-4Cr-*x*Zr (*x* = 2, 3, 4) alloys decreased with an increasing amount of Zr. The high tensile strength and elongation for all aged specimens can attribute to many α phases formed after the aging treatment, which act as inhibitors of dislocation motion in interface boundaries between the β and α phases. The co-existence of α phases could also induce a slightly improved elongation in the aged Ti-4Mo-4Cr-X (X = V, Sn, Zr) alloys. The highest value of elongation multiplied tensile strength (MPa × %) was 5.9 × 10^4 for the Ti-4Mo-4Cr-4Sn alloy, which was increased up to 22% after aging processing. As known Ti-Sn equilibrium phase diagram, the Sn containing alloy system has some intermetallic phases such as Ti_3Sn or Ti_2Sn, which cause

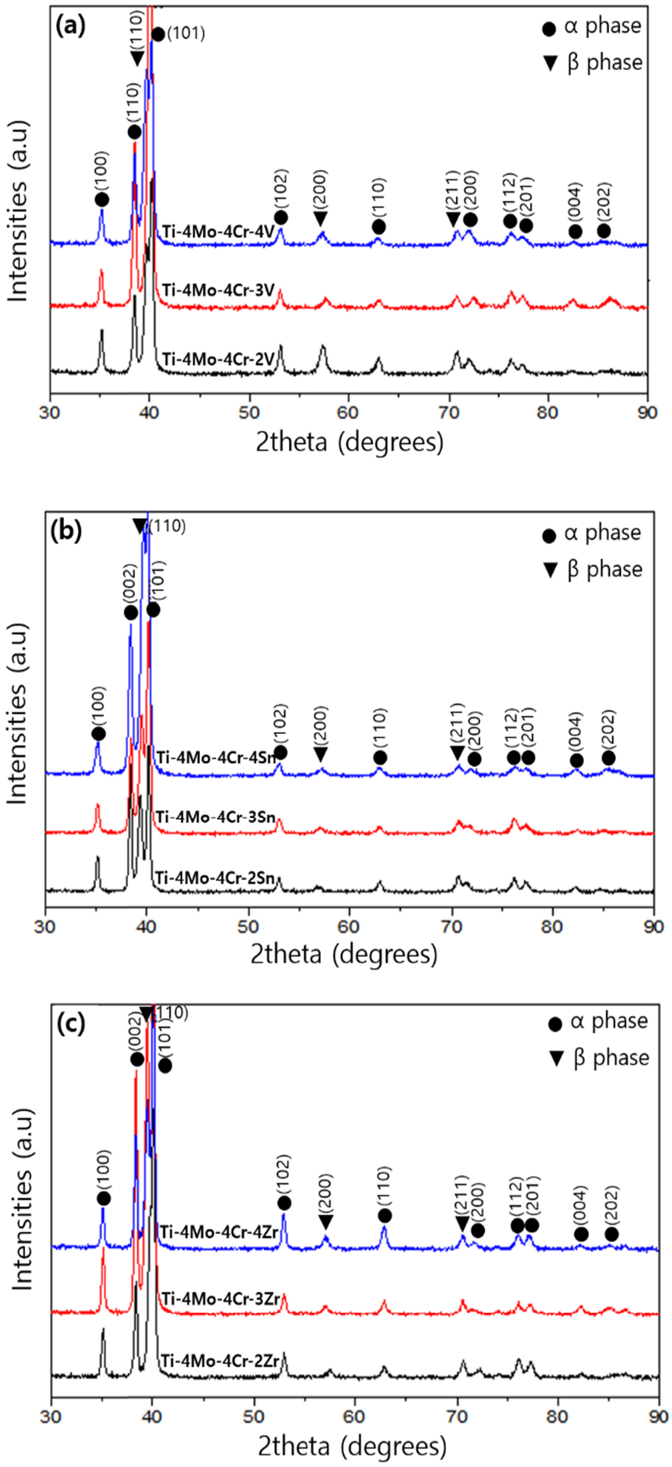

Fig. 1. XRD patterns of (a) Ti-4Mo-4Cr-*x*V (*x* = 2, 3, 4) alloys, (b) Ti-4Mo-4Cr-*x*Sn (*x* = 2, 3, 4) alloys, and (c) Ti-4Mo-4Cr-*x*Zr (*x* = 2, 3, 4) alloys, which were homogenized at 850°C for 4 h and subsequent aging treated at 450°C for 16 h

high tensile strength. Consequently, the aged Ti-4Mo-4Cr-4Sn alloy could be considered as an alloy candidate for the strength-ductility trade-off.

Fig. 3 shows SEM fractography of the aged (a) Ti-4Mo-4Cr-3V, (b) Ti-4Mo-4Cr-3Sn and (c) Ti-4Mo-4Cr-3Zr alloys after the tensile test. All aged Ti-4Mo-4Cr-3X (X = V, Sn, Zr) alloys after the tensile test showed a ductile fracture with

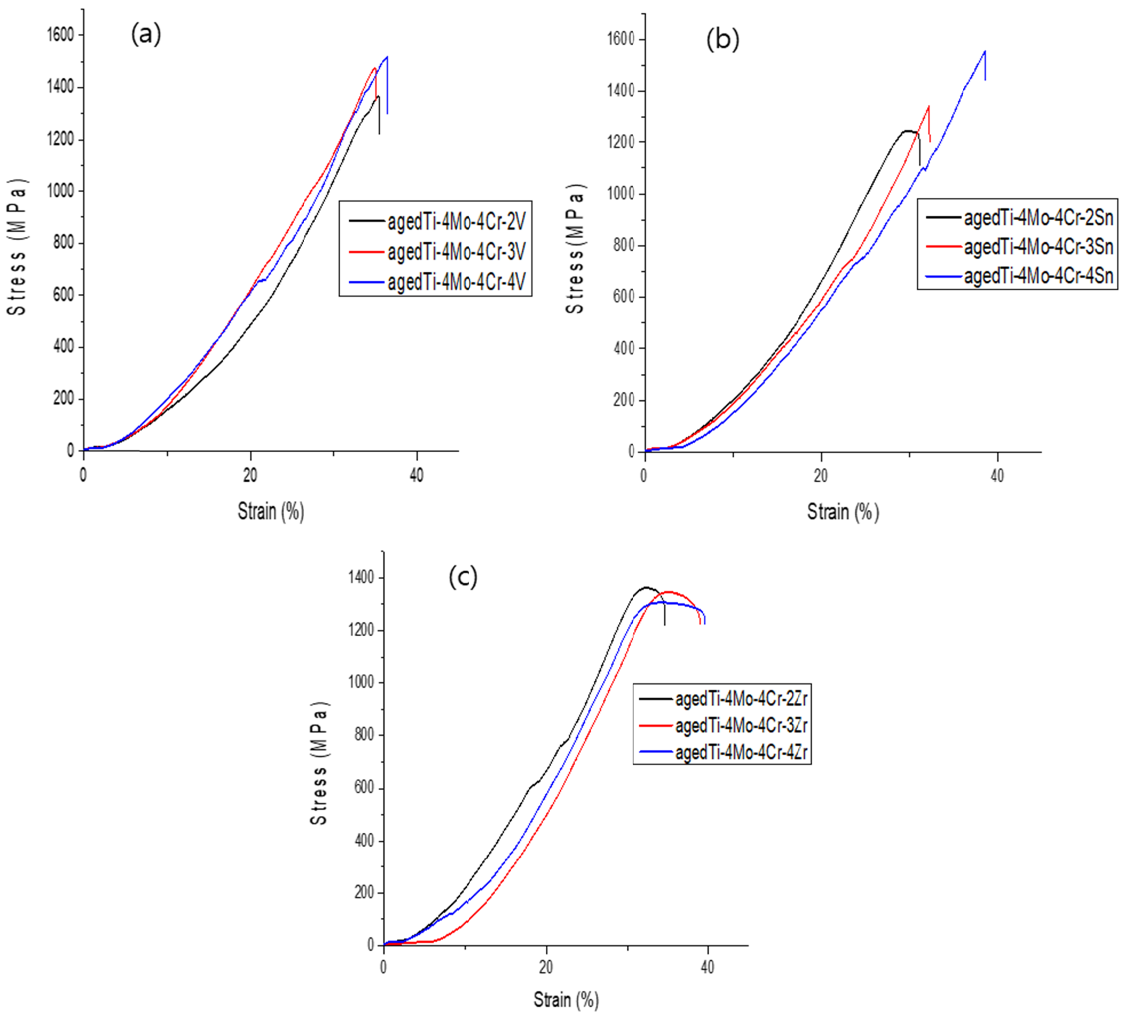

Fig. 2. Stress-strain curves after tensile tests of (a) Ti-4Mo-4Cr-*x*V (*x* = 2, 3, 4) alloys, (b) Ti-4Mo-4Cr-*x*Sn (*x* = 2, 3, 4) alloys, and (c) Ti-4Mo-4Cr-*x*Zr (*x* = 2, 3, 4) alloys, which were homogenized at 850°C for 4 h and subsequent aging treated at 450°C for 16 h

an elongation greater than 30% (31-39%). In Fig. 3, many fine dimple structures of less than 10 mm were observed in the alloy.

Fig. 4 shows the potentiodynamic polarization curves of the Ti-4Mo-4Cr-X (X = V, Sn, Zr) alloys as a function of the addition of an alloying element. Corrosion behaviors relating to biocompatibility are the main factors in a cardiovascular stent. In general, E_{corr} and i_{corr} represent the corrosion potential and corrosion current density, respectively. The lowest current density (1.05×10^{-8} A/cm^2) was observed in the Ti-4Mo-4Cr-4Sn alloy, whereas the specimen with the Ti-4Mo-4Cr-2Zr alloy showed the highest corrosion current density of 2.33×10^{-7} A/cm^2. As shown in the polarization graph, a passive layer on all the specimens was formed at a slow rate. The values of E_{corr} and i_{corr} for Ti-4Mo-4Cr-X (X= V or Sn) were found to be in the range of –0.032 and –0.317 V and the order of 10^{-8} A/cm^2, respectively. Basically, the addition of Mo and Cr elements to Ti alloys results in an improved corrosion resistance because of the formation of a passive films of TiO_2 and MoO_3 [7] and the formation of a chromium oxide-rich surface film in a fluoride-containing saline solution [8]. The Ti-4Mo-4Cr-X (X= V or Sn) alloys also showed an improved corrosion resistance with the exception of the Ti-4Mo-4Cr-*x*Zr (*x* = 2, 3, 4) alloys. However, in comparison with those of the available cardiovascular stent materials such as 316L stainless steel and L605 alloy, the corrosion resistance of the beta-type aged Ti-4Mo-4Cr-X (X = V, Sn, Zr) quaternary alloys appeared to be superior.

4. Conclusion

In this study, the mechanical properties and corrosion behaviors in Ringer's solution of a beta-type aged Ti-4Mo-4Cr-X (X = V, Sn, Zr) quaternary alloy were investigated. The following results were derived from this study.

1. 4th alloying elements, V as a β-phase stabilizing element and Sn or Zr as a α-phase stabilizing element, significantly affected the degree to which the volume of each phase could exist in quaternary Ti-4Mo-4Cr-X (X = V, Sn, Zr) alloys. The formation of the α phase after aging treatment contributed to an increase in the tensile strength and elongation of the alloy because the interface boundaries between the β and α phases can act as inhibitors of dislocation motion.

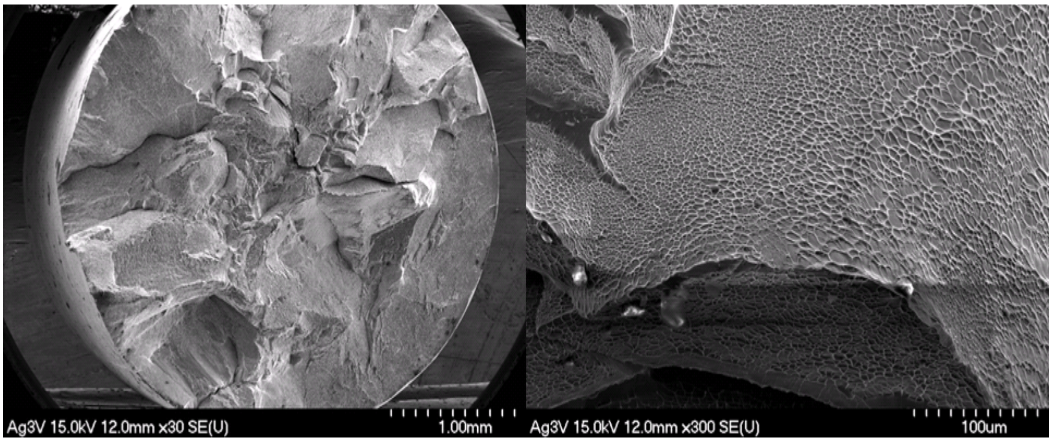

(a)

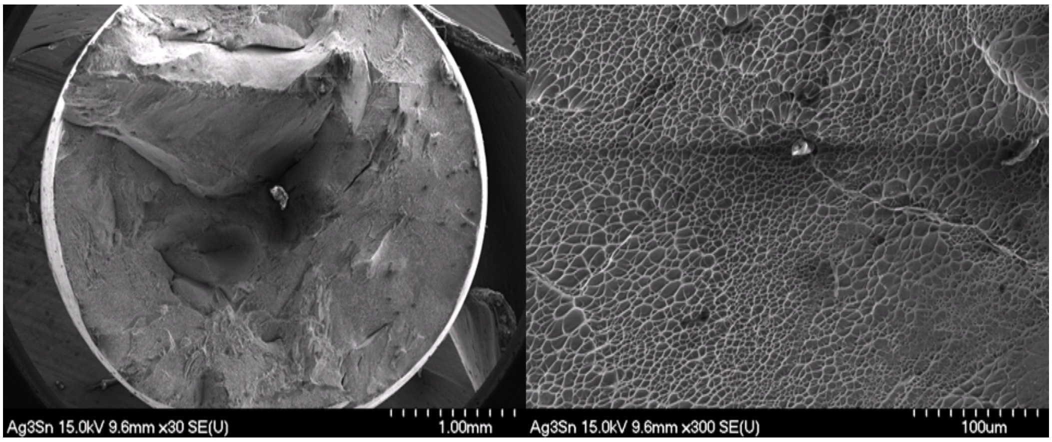

(b)

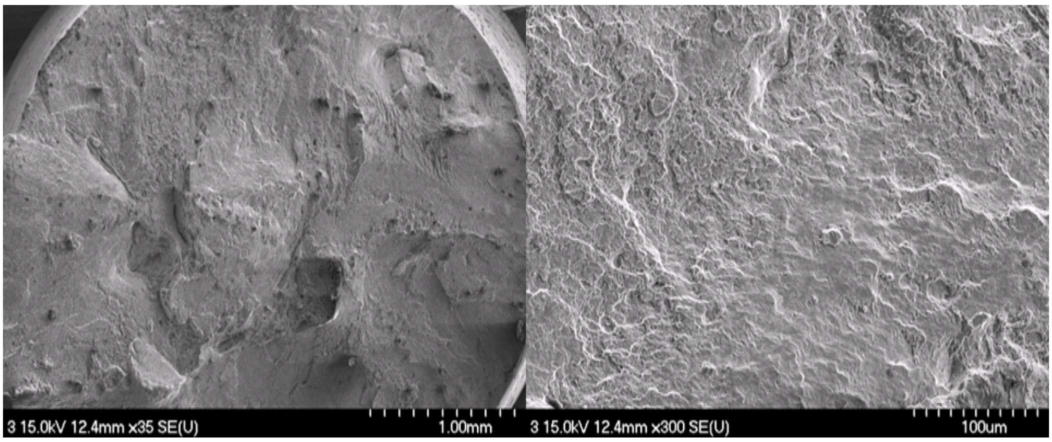

(c)

Fig. 3. SEM fractography of the aging treated Ti-4Mo-4Cr-X alloys after tensile tests: (a) Ti-4Mo-4Cr-3V, (b) Ti-4Mo-4Cr-3Sn and (c) Ti-4Mo-4Cr-3Zr

2. The tensile strength and elongation of the aged Ti-4Mo-4Cr-X (X = V, Sn, Zr) alloys increased as compared to the homogenized Ti-4Mo-4Cr-X (X = V, Sn, Zr) alloys. The aged Ti-4Mo-4Cr-4Sn alloy can be considered a Ti-alloy candidate for the strength-ductility trade-off.
3. Result of a polarization potential test revealed that the lowest current density of Ti-4Mo-4Cr-4Sn with 1.05×10^{-8} A/cm^2 was obtained. The studied Ti-4Mo-4Cr-X (X = V, Sn, Zr) alloys showed better corrosion characteristics as compared to the available cardiovascular stent materials such as 316L stainless steel and L605 (Co–Cr) alloy.

Acknowledgments

This research was supported by the Basic Science Research Program of the National Research Foundation of Korea (NRF) funded by the Ministry of Education (No. 2015R1D1A1A01056861).

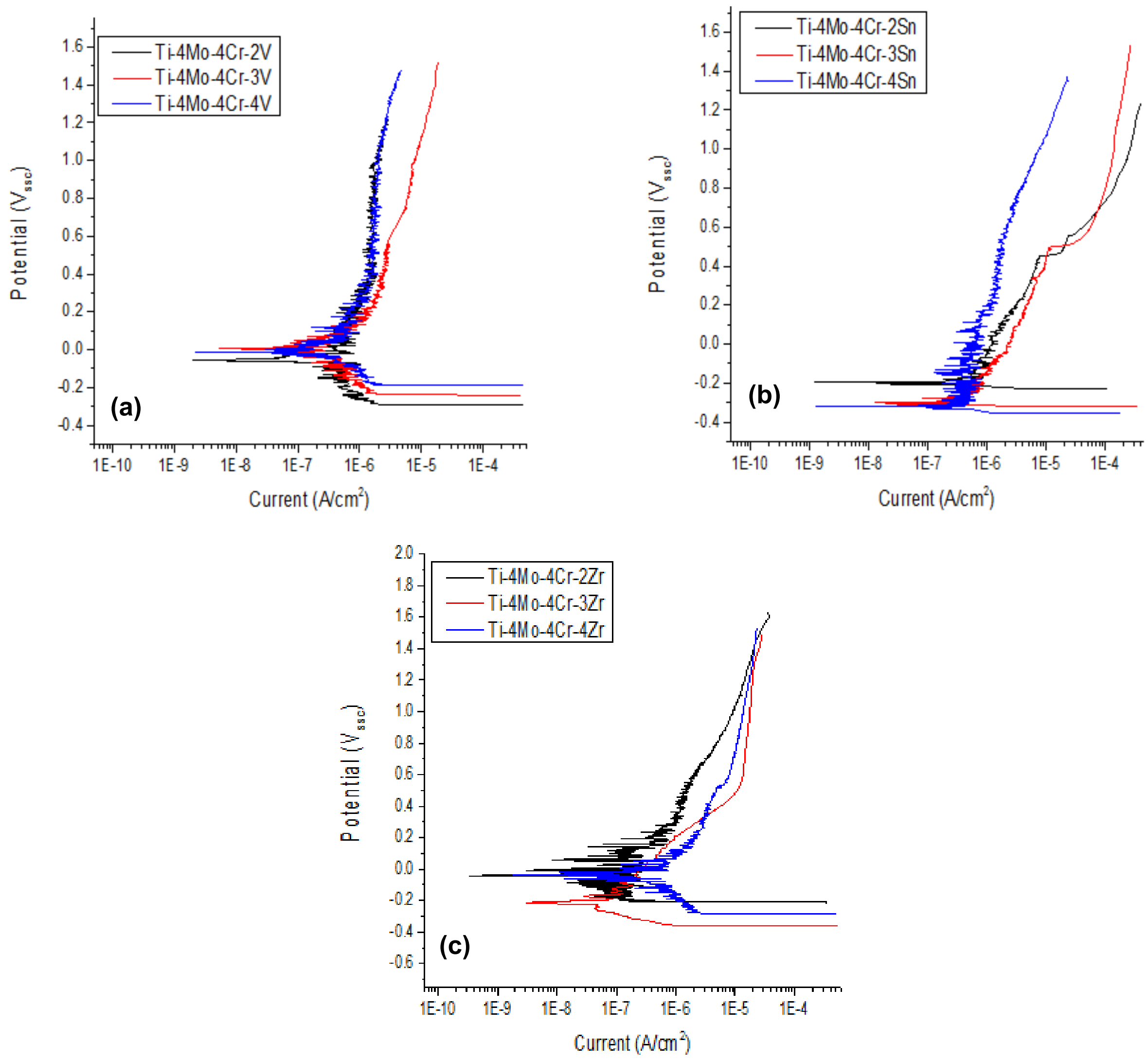

Fig. 4. Potentiodynamic polarization curves of (a) Ti-4Mo-4Cr-*x*V (*x* = 2, 3, 4) alloys, (b) Ti-4Mo-4Cr-*x*Sn (*x* = 2, 3, 4) alloys, and (c) Ti-4Mo-4Cr-*x*Zr (*x* = 2, 3, 4) alloys

TABLE 1

E_{corr} and i_{corr} values obtained at potentiodynamic polarization curves of Fig. 4

	Ti-4Mo-4Cr-xV (wt.%)			**Ti-4Mo-4Cr-xSn (wt.%)**			**Ti-4Mo-4Cr-xZr (wt.%)**		
	2	3	4	2	3	4	2	3	4
$E_{corr}(V_{ssc})$	–0.053	–0.039	–0.032	–0.196	–0.264	–0.317	–0.002	–0.170	–0.044
$I_{corr}(A/cm^2)$	2.79×10^{-8}	5.33×10^{-8}	8.75×10^{-8}	4.64×10^{-8}	1.62×10^{-8}	1.05×10^{-8}	2.33×10^{-7}	2.74×10^{-8}	1.04×10^{-7}
Control	**316L Stainless Steel**					**L605 Alloy (Co-20Cr-15W-10Ni) (wt.%)**			
$E_{corr}(V_{ssc})$	–0.564					–0.751			
$I_{corr}(A/cm^2)$	1.30×10^{-7}					2.29×10^{-5}			

REFERENCES

[1] J. Zhang, F. Sun, Y. Hao, N. Gozdecki, E. Lebrun, P. Vermaut, R. Portier, T. Gloriant, P. Laheurte, F. Prima, Mater. Sci. Eng. **A 563**, 78-85 (2013).

[2] G. Mani, M.D. Feldman, D. Patel, C.M. Agrawal, Biomater. **28**, 1689 (2007).

[3] Y. Song, D.S. Xu, R. Yang, D. Li, W.T. Wu, Z.X. Guo, Mater. Sci. Eng. **A 260**, 269 (1999).

[4] Y.L. Yang, W.Q. Wang, F.L. Li, W.Q. Li, Y.Q. Zhang, Mater. Sci. Forum, **618-619**, 169-172 (2009).

[5] R. Filip, K. Kubiak, W. Ziaja, J. Sieniawski, J. Mater. Process. Technol. **133**, 84 (2003).

[6] B. Vrancken, L. Thijs, J.-P. Kruth, J. Van Humbeeck, J. Alloy Compd. **541**, 177 (2012).

[7] Y. L. Zhou, D.M. Luo, J. Alloy Compd. **509**, 6267 (2011).

[8] S. Takemoto, M. Hattori, M. Yoshinari, E. Kawada, K. Asami, Y. Oda, Dent. Mater. **25**, 467 (2009).